



Published in final edited form as:

Anal Chem. 2012 April 17; 84(8): 3489–3492. doi:10.1021/ac300564g.

Stabilizing Nanometer Scale Tip-to-Substrate Gaps in Scanning Electrochemical Microscopy Using Isothermal Chamber for Thermal Drift Suppression

Jiyeon Kim, Mei Shen, Nikoloz Nioradze, and Shigeru Amemiya*

Department of Chemistry, University of Pittsburgh, Pittsburgh, Pennsylvania 15260

Abstract

The control of a nanometer-wide gap between tip and substrate is critical for nanoscale applications of scanning electrochemical microscopy (SECM). Here we demonstrate that the stability of the nanogap in ambient conditions is significantly compromised by the thermal expansion and contraction of components of an SECM stage upon a temperature change and can be dramatically improved by suppressing the thermal drift in a newly developed isothermal chamber. Air temperature in the chamber changes only at ~ 0.2 mK/min to remarkably and reproducibly slow down the drift of tip–substrate distance to ~ 0.4 nm/min in contrast to 5–150 nm/min without the chamber. Eventually, the stability of the nanogap in the chamber is limited by its fluctuation with a standard deviation of ± 0.9 nm, which is mainly ascribed to the instability of a piezoelectric positioner. The sub-nanometer scale drift and fluctuation are measured by forming a ~ 20 nm-wide gap under the 12 nm-radius nanopipet tip based on ion transfer at the liquid/liquid interface. The isothermal chamber is useful for SECM and, potentially, for other scanning probe microscopes, where thermal-drift errors in vertical and lateral probe positioning are unavoidable by the feedback-control of the probe–substrate distance.

Scanning electrochemical microscopy (SECM)^{1,2} serves as a powerful nanoelectrochemical method with high spatial/time resolutions and superb sensitivity when a gap between tip and substrate is narrowed to nanometer scale. A nanoscale tip–substrate distance is required for operating a nanometer-sized SECM tip in the feedback mode to enable the imaging of substrate reactivity and/or topography with nanometer resolutions^{3–6} and the kinetic measurements of rapid charge-transfer reactions at metal nanotips^{7,8} or at liquid/liquid interfaces^{9,10} under high mass transport conditions. Also, nanoscale SECM allows for the positive-feedback detection of a single electroactive molecule, which repeatedly undergoes electron-transfer reactions at the nanotip held at a few nanometers from a conductive substrate.^{11–14} On the other hand, a micrometer-sized tip can be also used to form a nanogap over a much larger substrate as demonstrated in the kinetic study of rapid electron-transfer reactions.^{15–17} In addition to a higher mass transport condition, the advantage of the nanogap against a conventional micrometer-wide gap is that a transient electron-transfer reaction at a macroscopic substrate can be investigated in the wide range of substrate potentials under quasi-steady states in either feedback or substrate generation/tip collection mode.^{16,18} Moreover, an extremely short-lived intermediate can be generated and detected by forming a nanogap between two micrometer-sized electrodes with a thin insulating sheath.¹⁹

*To whom correspondence should be addressed. amemiya@pitt.edu.

Supporting Information Available. Additional information as noted in text. This material is available free of charge via the Internet at <http://pubs.acs.org>.

Here, we report on the novel approach based on an isothermal chamber to dramatically and reproducibly slow down the thermal drift of nanometer scale tip–substrate gaps to sub-nanometer-per-minute levels, which are required for facilitating the aforementioned nanoscale applications of SECM or enabling them at a smaller scale. In fact, this work is the first to demonstrate that the minute-long stability of the nanogaps is limited to nanometer or sub-micrometer levels by the thermal expansion and contraction of components of an SECM stage as driven by a temperature change. In a previous SECM study, such a change in tip–substrate distance was ascribed to the drift of a piezoelectric positioner.²⁰ Importantly, the thermal drift has been recognized as the origin of vertical and lateral image distortions and unstable nanomanipulation in other scanning probe microscopy techniques even when the probe–substrate distance is feedback-controlled.^{21,22} Currently, these problems due to thermal drift is unavoidable, unless a cryostat or fast scanning is employed, and is only correctable,²³ thereby augmenting the significance of our approach for the reduction of thermal-drift errors in tip positioning to sub-nanometer levels.

The significant drift of tip–substrate distance in the ambient environment of our laboratory was confirmed without the isothermal chamber when a tip was positioned at a feedback distance of <1 μm from a substrate and the feedback tip current was measured without any lateral tip scan, which minimizes the effect of substrate tilt on the tip current. For instance, Figure 1a shows the time profile of a current response at a 0.44 μm -radius Pt tip with a 0.22 μm -thick glass sheath as fabricated elsewhere¹⁶ when the tip was brought to and positioned at 0.11 μm from the surface of a SiO_2/Si wafer. The width of a tip–substrate gap, d , as well as inner and outer tip radii (a and r_g , respectively) were determined from the good fit of the tip current, i_T , with the theoretical negative feedback current as given by²⁴

$$\frac{i_T}{i_{T,\infty}} = \frac{\frac{2.08}{RG^{0.358}} \left(L - \frac{0.145}{RG} \right) + 1.585}{\frac{2.08(L+0.0023RG)}{RG^{0.358}} + 1.57 + \frac{\ln RG}{L} + \frac{2}{\pi RG} \ln \left(1 + \frac{\pi RG}{2L} \right)} \quad (1)$$

with

$$i_{T,\infty} = 4xnFDc^*a \quad (2)$$

where $RG = r_g/a$, $L = d/a$, $i_{T,\infty}$ is the diffusion-limited tip current in the bulk solution, x is a function of RG , n is the number of transferred charges in the tip reaction, and D and c^* are the diffusion coefficient and concentration of the original mediator in the bulk solution. Noticeably, a tip approach rate of 83.3 nm/s was used to convert the tip–substrate distance in eq 1 to time in Figure 1a. As soon as the tip approach was stopped, the tip current gradually increased to nearly completely recover to $i_{T,\infty}$ within ~ 10 minutes, where negative feedback effect became almost negligible. This result indicates that the tip–substrate gap became wider without moving a z -axis piezoelectric positioner. Quantitatively, the tip–substrate distance increased at ~ 100 nm/min in < 10 minutes (Figure 1b) as calculated from the tip current using the following approximate equation for the inverse function of eq 1

$$L = \left(2.35 \times 10^{-2} \right) \exp \left(6.99 i_T / i_{T,\infty} \right) - \left(3.5 \times 10^{-5} \right) \exp \left(13.3 \sqrt{i_T / i_{T,\infty}} \right) \quad (3)$$

where $RG = 1.5$ was employed.

We repeatedly monitored the time profile of feedback tip current as the measure of tip–substrate distance without vertical or lateral tip scan on different days to find that the gap

becomes either wider or narrower at drift rates in the wide range of 5–150 nm/min. Such drift rates were obtained using the 0.5 μm -radius tip of either Pt or interface between two immiscible electrolyte solutions (ITIES) at the tip of a micropipet.²⁵ A total drift of up to 1 μm is too large to be ascribed to the hysteresis or creep of a piezoelectric positioner with a capacitive position sensor, which was operated in the closed-loop mode using an amplifier/servo controller. Similar drift rates were also obtained using an inchworm motor without closed-loop control (see Supporting Information). Overall, these results are consistent with our finding that the drift of tip–substrate distance is predominantly thermal (see below).

To suppress thermal drift, we developed an isothermal chamber (Figure 2) with a temperature stability of ~ 0.2 mK/min, which is comparable to that of <250 mK for 24 hours, i.e., <0.17 mK/min, in the laboratory where the closed-loop piezoelectric positioner is calibrated by its manufacturer at the sub-nanometer scale.²⁶ In addition, a ~ 10 cm-height SECM stage with a typical coefficient of linear thermal expansion in the order of 10^{-5} K^{-1} is expected to expand or contract only by 0.2 nm for a temperature change of 0.2 mK.²³ Specifically, we thermally isolated an SECM stage from the ambient environment using the box of the vacuum insulated panels (VIPs) based on a porous solid with pore sizes ranging from 10–100 nm, which are ~ 5 – 8 times thermally more resistive than polystyrene and polyurethane foams with the same thickness.²⁷ Additionally, the SECM stage was surrounded by extruded aluminum heat sinks to quickly absorb excess heat from air in the chamber, which was heated by an operator and an illumination during the setup of SECM tip and cell. Also, the opening of the SECM solution cell was sealed with a rubber cap only with a small hole for the insertion of an SECM tip (Figure S-1a), thereby reducing cooling due to solvent evaporation. Finally, the chamber was closed with a VIP (Figure S-1b) and then tightly sandwiched between aluminum plates (Figure S-1c) to squeeze any gap between VIPs.

The stable air temperature in the chamber was determined using a thermometer with a high resolution of 0.1 mK. Upon the closure of the chamber, the temperature typically increased, reached to a plateau within 10 minutes, and decreased only at ~ 0.2 mK/min for an hour (Figure 3). This decrease in the chamber temperature is likely due to the slow exchange of air between inside and outside of the chamber through gaps between VIPs and also through the holes for cables drilled in the neoprene foam (Figures 2 and S-1a). On the other hand, the increase in the temperature upon the closure of the chamber is likely due to the self-heating of the thermometer,²⁸ which is noticeable when air convection is suppressed in the closed chamber. The thermometer self-heating, however, was so local and weak that the stability of tip–substrate distance was unaffected by turning on or off the thermometer. Importantly, the achievement of the stable chamber temperature also requires the reduction of heating by an operator and the quick removal of the excess heat. Some care was taken (see Supporting Information for details) to minimize the temperature rise to 0.3 $^{\circ}\text{C}$ during the setting up of SECM tip and cell (Figure 3). After the operator completed the setup and left the chamber, the temperature more quickly decreased because the excess heat in the chamber was absorbed by the aluminum heat sinks.

The sub-nanometer stability of a tip–substrate nanogap in the isothermal chamber was demonstrated using a nanopipet-supported ITIES tip²⁹ (see Supporting Information for nanopipet fabrication and SECM measurements). In Figure 4a, an $i_{T,\infty}$ value of 52 pA is based on the transfer of tetraethylammonium across the ITIES formed at the tip of a 1,2-dichloroethane-filled nanopipet, thereby yielding a tip radius of 12 nm in eq 2 with a typical RG value of ~ 1.5 . The tip inner and outer radii were also confirmed by the good fit of eq 1 with the nanopipet approach curve at the insulating surface, where a tip approach rate of 10.0 nm/s was used to convert the tip–substrate distance in eq 1 to time in Figure 4a. After the tip was stopped at 22.3 nm from the SiO_2/Si wafer surface, the tip current decreased only

by ~ 3 pA for 10 minutes, which is larger than the decrease of $i_{T,\infty}$ at the tip far away from a substrate (typically a decrease of ~ 1.5 pA at a 12 nm-radius tip for 10 minutes). The tip current in Figure 4a was converted to the tip–substrate distance using eq 3 (Figure 4b) to estimate a decrease of 4.6 nm in the distance. A drift rate of -0.44 nm/min was obtained from the linear fit of the distance versus time plot (red line in Figure 4b). Remarkably, this drift rate is 11–340 times lower than that without the chamber and is comparable to or better than that of 0.6–6 nm/min as reported for electrochemical scanning tunneling microscopy/spectroscopy.³⁰ Noticeably, the sub-nanometer scale drift of a tip–substrate gap requires the operation of the piezoelectric positioner in the drift compensation mode,³¹ which eliminates the drift of digital-analog converters on the main board of the controller.

Eventually, the stability of a tip–substrate gap in the isothermal chamber is limited by the sub-nanometer scale fluctuation of the gap, which results in noisier tip current at feedback distances than in the bulk solution (Figure 4a). The corresponding distance fluctuation with respect to the best linear fit in Figure 4b gives a standard deviation of ± 0.9 nm. This fluctuation is mainly ascribed to the instability of the piezoelectric positioner, where the capacitive sensor gave relative piezo positions with a standard deviation of ± 0.4 nm (Figure S-2). Such piezo fluctuation is negligible in comparison to typical tip–substrate distances of 0.1–1 μm at a 0.5 μm -radius tip,¹⁶ which is seen as smooth feedback current without a chamber in Figure 1. Subsequently, the feedback current at the 0.5 μm -radius tip of Pt or micropipet-supported ITIES in the isothermal chamber showed negligible drift and fluctuation (data not shown).

CONCLUSIONS

The sub-nanometer scale stability of tip–substrate nanogaps with a drift rate of ~ 0.4 nm/min and a fluctuation of ~ 0.9 nm was achieved using the newly developed isothermal chamber with a temperature drift rate of only ~ 0.2 mK/min. This achievement is highly significant for facilitating nanoscale SECM measurements or enabling them at the smaller scale. In contrast, the thermal drift of the gap width without the chamber is much more significant and strongly depends on ambient conditions to vary in the wide range of 5–150 nm/min. This finding explains why the holding of a tip at a constant feedback distance of < 1 μm for > 1 min in imaging^{32,33} and voltammetry¹⁶ is sometimes very difficult in ambient conditions without the chamber. Thermal drift is much less problematic in approach curve measurements even with a < 10 nm-radius tip,³⁴ which travels the whole feedback distance within seconds. Noticeably, the thermal drift effect may be very different in other laboratories and with different SECM instruments and can be assessed simply by monitoring the feedback tip current without tip movement.

Our approach based on the isothermal chamber is robust and general because this approach is effective to tips and substrates with various sizes and materials.^{1,2} The thermal drift of a tip–substrate gap in this chamber will be further suppressible by better designing an SECM stage including its dimensions and compositions while a more stable piezoelectric positioning system is required for the reduction of gap fluctuation. Noticeably, maintaining a constant tip–substrate distance using a distance-dependent feedback signal can not avoid lateral and topographic distortions of an image due to thermal drift.^{21,22} Our isothermal chamber will be useful for the reduction of thermal drift in various scanning probe microscopic techniques and also for such isothermal measurements as the long-term measurement of the temperature-sensitive resonance frequency of a quartz crystal microbalance.³⁵

Supplementary Material

Refer to Web version on PubMed Central for supplementary material.

Acknowledgments

This work was supported by grants from the National Institutes of Health (GM073439). We thank Prof. Patrick R. Unwin, Department of Chemistry, University of Warwick, for his valuable comments on thermal drift.

References

1. Bard, A.J.; Mirkin, M.V., editors. Scanning Electrochemical Microscopy. Marcel Dekker; New York: 2001.
2. Amemiya S, Bard AJ, Fan FRF, Mirkin MV, Unwin PR. *Ann Rev Anal Chem.* 2008; 1:95.
3. Fan FRF, Bard AJ. *Proc Natl Acad Sci USA.* 1999; 96:14222. [PubMed: 10588687]
4. Sun P, Laforge FO, Abeyweera TP, Rotenberg SA, Carpino J, Mirkin MV. *Proc Natl Acad Sci USA.* 2008; 105:443. [PubMed: 18178616]
5. Laforge FO, Velmurugan J, Wang Y, Mirkin MV. *Anal Chem.* 2009; 81:3143. [PubMed: 19281245]
6. Takahashi Y, Shevchuk AI, Novak P, Zhang Y, Ebejer N, Macpherson JV, Unwin PR, Pollard AJ, Roy D, Clifford CA, Shiku H, Matsue T, Klenerman D, Korchev YE. *Angew Chem, Int Ed.* 2011; 50:9638.
7. Sun P, Mirkin MV. *Anal Chem.* 2006; 78:6526. [PubMed: 16970330]
8. Velmurugan J, Sun P, Mirkin MV. *J Phys Chem C.* 2008; 113:459.
9. Sun P, Zhang ZQ, Gao Z, Shao YH. *Angew Chem, Int Ed.* 2002; 41:3445.
10. Li F, Chen Y, Sun P, Zhang MQ, Gao Z, Zhan DP, Shao YH. *J Phys Chem B.* 2004; 108:3295.
11. Fan FRF, Bard AJ. *Science.* 1995; 267:871. [PubMed: 17813918]
12. Bard AJ, Fan FRF. *Acc Chem Res.* 1996; 29:572.
13. Fan FRF, Kwak J, Bard AJ. *J Am Chem Soc.* 1996; 118:9669.
14. Sun P, Mirkin MV. *J Am Chem Soc.* 2008; 130:8241. [PubMed: 18540603]
15. Mirkin MV, Richards TC, Bard AJ. *J Phys Chem.* 1993; 87:7672.
16. Nioradze N, Kim J, Amemiya S. *Anal Chem.* 2011; 83:828. [PubMed: 21175129]
17. Shen M, Bard AJ. *J Am Chem Soc.* 2011; 133:15737. [PubMed: 21842886]
18. Amemiya S, Nioradze N, Santhosh P, Deible MJ. *Anal Chem.* 2011; 83:5928. [PubMed: 21682337]
19. Bi S, Liu B, Fan FRF, Bard AJ. *J Am Chem Soc.* 2005; 127:3690. [PubMed: 15771491]
20. O'Mullane AP, Macpherson JV, Unwin PR, Cervera-Montesinos J, Manzanares JA, Frehill F, Vos JG. *J Phys Chem B.* 2004; 108:7219.
21. Moheimani SOR. *Rev Sci Instrum.* 2008; 79:071101. [PubMed: 18681684]
22. Marinello F, Balcon M, Schiavuta P, Carmignato S, Savio E. *Meas Sci Technol.* 2011; 22:094016.
23. Rahe P, Bechstein R, Kuhnle A. *J Vac Sci Technol, B.* 2010; 28:C4E31.
24. Lefrou C. *J Electroanal Chem.* 2006; 592:103.
25. Ishimatsu R, Kim J, Jing P, Striemer CC, Fang DZ, Fauchet PM, McGrath JL, Amemiya S. *Anal Chem.* 2010; 82:7127. [PubMed: 20690617]
26. [accessed February 24, 2012] http://www.physikinstrumente.com/en/products/nanopositioning/test_calibration.php
27. [accessed February 24, 2012] <http://www.nanopore.com/vip.html>
28. Nicholas, J.V.; White, D.R. *Traceable Temperatures: An Introduction to Temperature Measurement and Calibration.* 2. Wiley and Sons; 2001. p. 223
29. Wang Y, Velmurugan J, Mirkin MV, Rodgers PJ, Kim J, Amemiya S. *Anal Chem.* 2010; 82:77. [PubMed: 20000449]
30. Hugelmann P, Schindler W. *J Phys Chem B.* 2005; 109:6262. [PubMed: 16851695]

31. PZ116E User Manual: E-816 Computer Interface and Command Interpreter Submodule for Piezo Controller. Physik Instrumente; Karlsruhe, Germany:
32. Xiong H, Gross DA, Guo J, Amemiya S. *Anal Chem.* 2006; 78:1946. [PubMed: 16536432]
33. Kim J, Xiong H, Hofmann M, Kong J, Amemiya S. *Anal Chem.* 2010; 82:1605. [PubMed: 20112959]
34. Elsamadisi P, Wang Y, Velmurugan J, Mirkin MV. *Anal Chem.* 2011; 83:671. [PubMed: 21162580]
35. Cimpoa GV, Radulescu C, Popescu IV, Dulama ID, Ionita I, Cimpoa M, Cernica I, Gavrilă R. *AIP Conf Proc.* 2010; 1203:160.

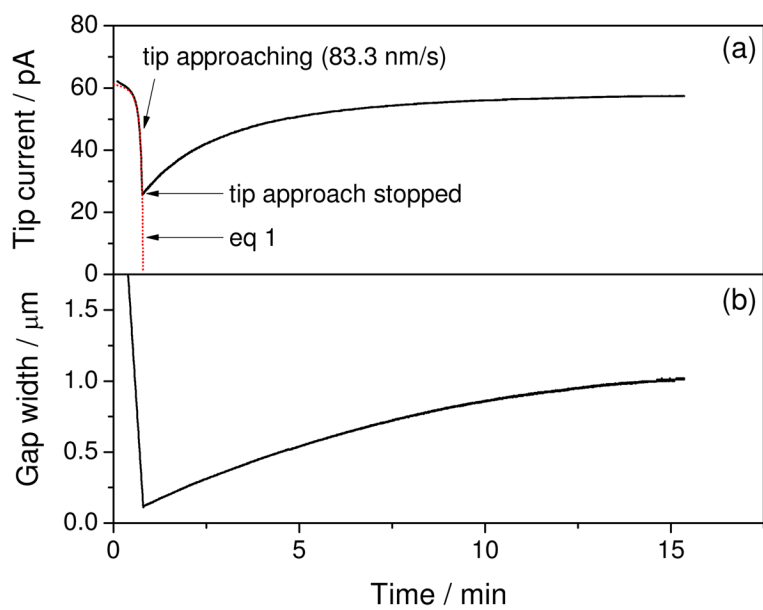


Figure 1. Time profile of (a) the tip current based on the oxidation of 0.5 mM ferrocenemethanol in 0.2 M NaCl without an isothermal chamber and (b) the corresponding width of the tip–substrate gap calculated using eq 3.

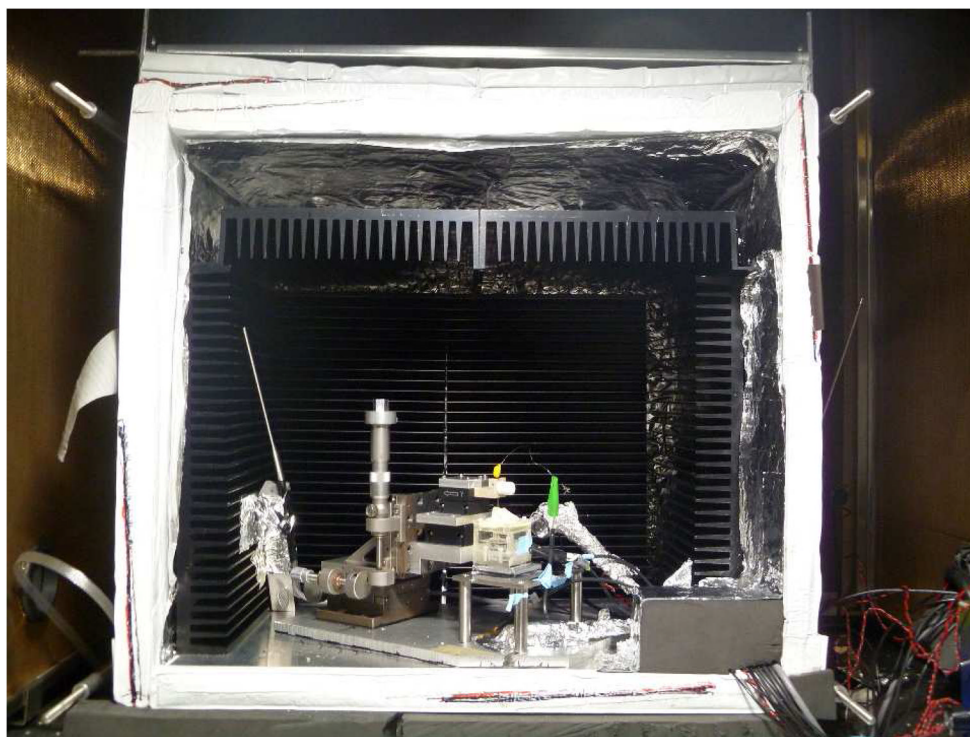


Figure 2. Image of an SECM stage in the isothermal chamber based on the box of VIPs (white) and extruded aluminum heat sinks (black). A thermometer is seen at the left-hand side of the stage while the neoprene foam (gray) is located at the right bottom corner. See Figure S-1a for details of the SECM stage and the capped cell.

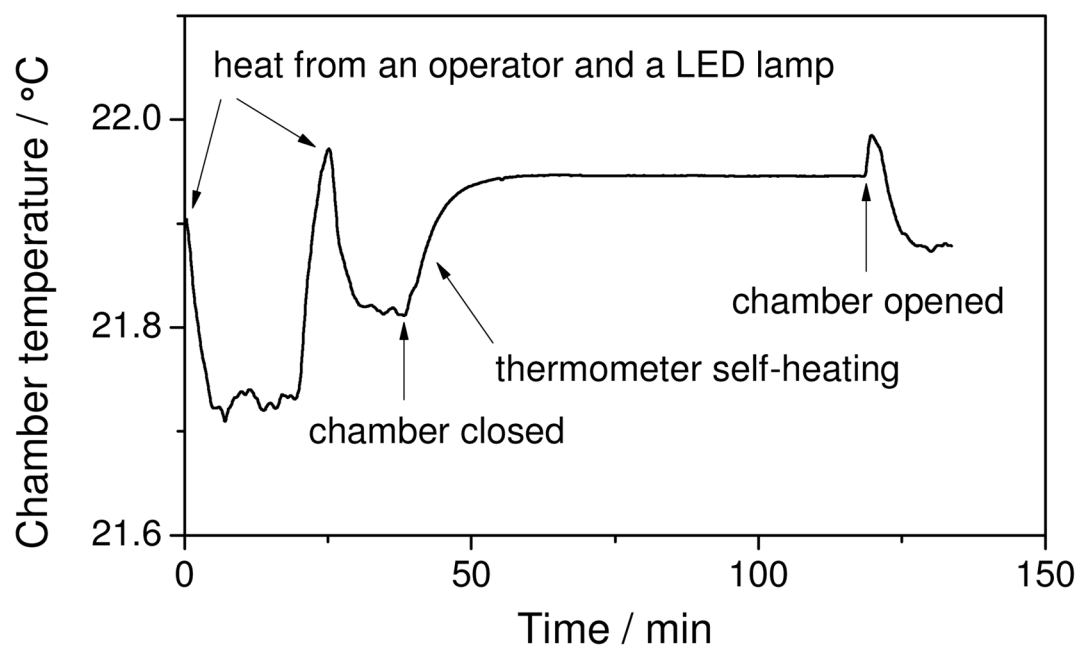


Figure 3.
Time profile of air temperature in the isothermal chamber.

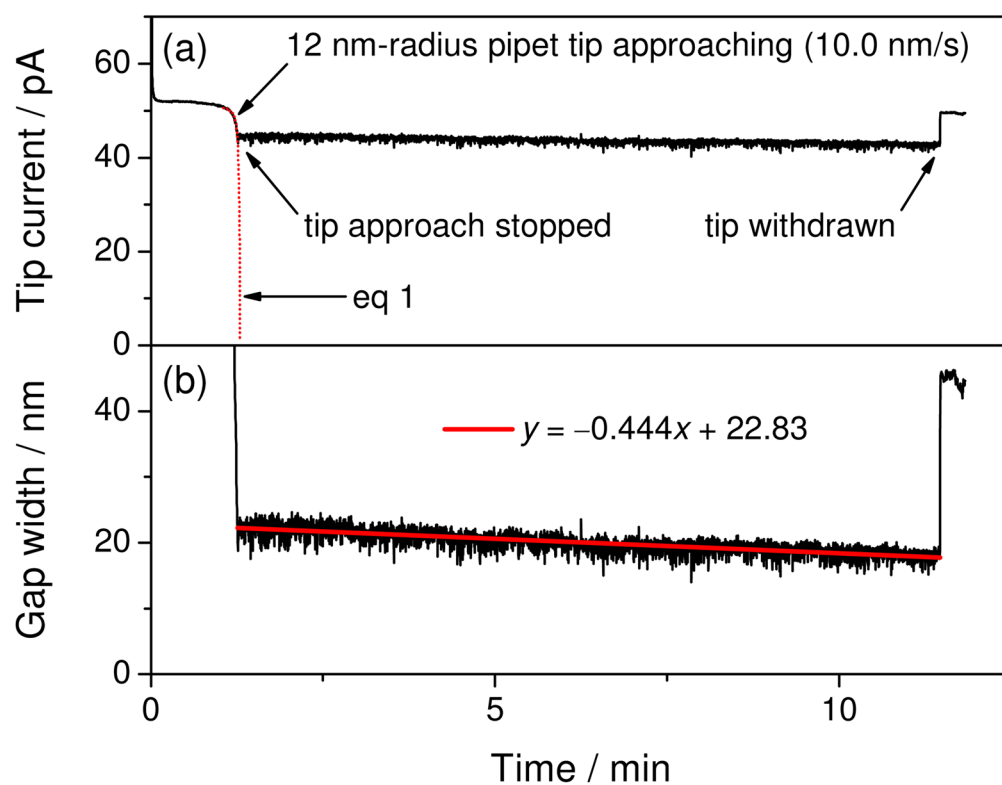


Figure 4. Time profile of (a) the tip current based on the transfer of 10 mM tetraethylammonium in 0.3 M KCl and (b) the corresponding tip–substrate gap width calculated using eq 3. Chamber temperature drifted at -0.2 mK/min during the current measurement.